Available online at www.sciencedirect.com
ScienceDirect
Journal of Nuclear Materials 367–370 (2007) 500–504
journal of nuclear materials
www.elsevier.com/locate/jnucmat

Effectiveness of helium bubbles as traps for hydrogen

S.Yu. Binyukova *, I.I. Chernov, B.A. Kalin, Than Swe

Moscow Engineering Physics Institute (State University), 31 Kashirskoye Sh., Moscow 115409, Russia

Abstract

Comparing ferritic–martensitic and austenitic steels, it is concluded that the austenitic steel with a uniform distribution of helium bubbles retain a greater quantity of hydrogen than the ferritic–martensitic steel with helium bubbles predominantly located on dislocations.

1. Introduction

Much attention is given to the effect of helium and hydrogen in materials during the development of fusion energy sources in view of their negative influence on the radiation resistance of structural materials. This may frequently be an important reason for degradation of their properties and shortening of the useful life of reactor structural components. There is also the issue of hydrogen penetration of the fusion reactor first wall in connection with tritium use, since the diffusion leakage may be considerable. In addition, a new effect has been found recently – the radiation swelling of vessel internals of thermal fission reactors at relatively low temperatures (about 570 K). Hypothetically, this effect is caused by hydrogen accumulation in the smallest pores stabilized by helium atoms [1,2].

The aim of this paper is to investigate the gas bubbles evolution and helium and hydrogen behavior in ferritic–martensitic and austenitic steels irradiated by He^+-ions at various temperatures (for creation of different pressures in helium bubbles) and subsequently by 25-keV H^+-ions at room temperature.

2. Experimental procedure

The samples of ferritic–martensitic Cr12MoWSiVNbNB (EP-900) and austenitic Cr18Ni10Ti steels were heat-treated by standard methods: normalization at 1370 K for 40 min, air cooling + tempering at 990 K for 3 h, air cooling for EP-900 steel and solution annealing at 1370 K for 40 min, air cooling for Cr18Ni10Ti steel.

Some of the samples were irradiated by 40-keV He^+-ions to a fluence of 5×10^{20} m^{-2} in the temperature range of $T_{irrad} = 270$–900 K for the purpose of creating helium porosity with different helium pressures in bubbles. Unirradiated samples and samples with previously created helium porosity were then implanted with 25-keV H^+-ions to a fluence of 5×10^{20} m^{-2} at room temperature. The projected range of H^+-ions was the same as for He^+-ions (about 0.15 μm). The samples were thinned from

* Corresponding author.
E-mail address: binu@phm.mephi.ru (S.Yu. Binyukova).

0022-3115/$ - see front matter © 2007 Published by Elsevier B.V.
doi:10.1016/j.jnucmat.2007.03.110

the unirradiated side and their microstructures were studied using a transmission electron microscope (TEM) JEM-2000EX. The hydrogen content was determined by the vacuum reducing melting method in a LECO high sensitivity gas analyzer, RH-402. The details of implanted helium desorption were studied using helium thermal desorption spectrometry (HTDS) (sensitivity 10^8–10^{10} at. He/s).

3. Results and discussion

Figs. 1 and 2 show typical microstructures of steels irradiated by He^+-ions at different temperatures. As can be seen from Table 1, the gas bubbles in EP-900 steel do not form up to 570 K. Helium in the crystal lattice is in the form of various helium–vacancy complexes [3–6]. After irradiation at 690 K bubbles were not observed either, although the presence of a specific contrast ratio in a through-focus sequence of the TEM-images [7] points to the possible presence of fine bubbles with sizes close to the resolution limit of TEM. The bubbles that can be fully resolved by TEM and having diameters of 0.5–1 nm and a volume density of the order of 10^{25} m^{-3} form only at 770 K. Their sizes increase and their densities sharply decrease with an increase of irradiation temperature up to 900 K (Fig. 2 and Table 1). A peculiar feature of bubbles formed at high temperature in EP-900 steel is their faceting and non-uniform distribution with a predominant location on dislocations (shown by arrows Fig. 2).

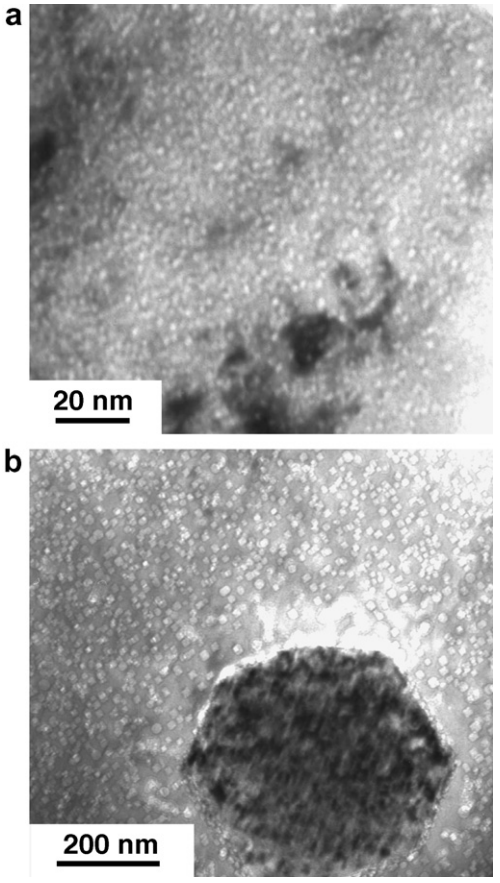

Fig. 1. Typical microstructure of Cr18Ni10Ti steel irradiated by He^+-ions at 690 (a) and 900 K (b).

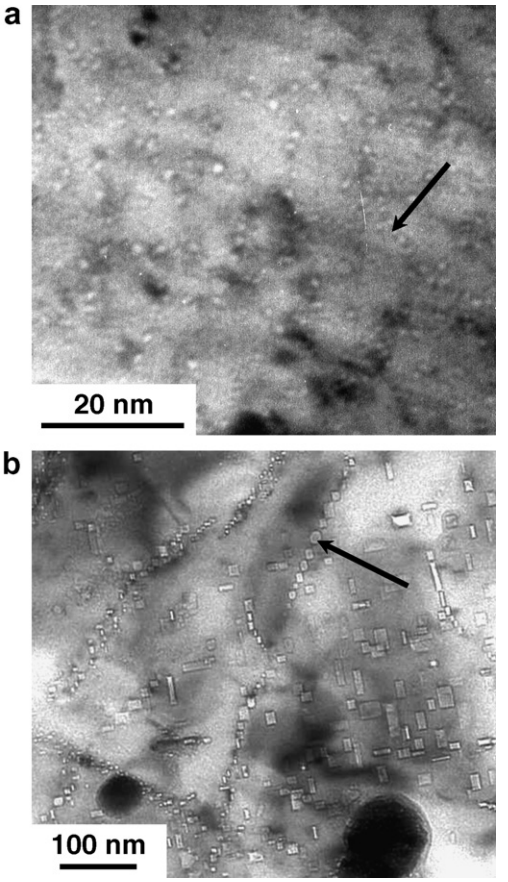

Fig. 2. Characteristic distribution of bubbles (predominant location of bubbles on dislocations is showed by arrows) in EP-900 steel irradiated by He^+-ions at 770 (a) and 900 K (b).

Through-focus of TEM imaging indicates the presence of unresolved bubbles in Cr18Ni10Ti steel is also possible at 570 K. In this steel the characteristic features of microstructure evolution are a uniform distribution of helium bubbles in the matrix and their spherical form at irradiation temperatures of 690 (Fig. 1(a)) and 770 K. The character of the

Table 1
The bubble parameters in Cr18Ni10Ti and EP-900 steels irradiated by He^+-ions at different temperatures

Steel	Irradiation temperature (K)	Maximum bubble diameter (nm)	Mean bubble diameter (nm)	Bubble concentration (10^{22} m^{-3})	Calculated swelling (%)	Ratio of gas quantity in bubbles to the total quantity of trapped helium
Cr18Ni10Ti	570	– (?)	– (?)	– (?)	– (?)	– (?)
	690	~4	1.6	79 ± 20	$0.25 \pm 0{,}06$	0.2
	770	~5	2.4	48 ± 12	0.43 ± 1.1	0.5
	900	~12	4.2	18 ± 5	1.7 ± 0.4	$\geqslant 1$
EP-900	570	–	–	–	–	–
	690	– (?)	– (?)	– (?)	– (?)	– (?)
	770	~1.5	~0.6	~1000	~0.03	0.2
	900	~24	8.2	2.7 ± 0.7	2.9 ± 0.7	1.7

helium bubble microstructure evolution changes at the maximum irradiation temperature of 900 K: large faceted bubbles form uniformly in the austenitic steel matrix, in contrast to bubbles forming on dislocations in ferritic–martensitic steel (see Figs. 1(b) and 2(b)). In addition, bubbles are observed on precipitate–matrix boundaries, and there are no bubbles in adjoining volumes (Fig. 1(b)).

It is known [1,2,8–10] that helium bubbles can trap implanted hydrogen, but the influence of the bubble distribution character and helium pressure in these bubbles on the quantity of trapped hydrogen is not clear. The calculated ratio according to [6,11] of the gas quantity in bubbles to the total quantity of trapped helium (N/N_0) is presented in Table 1. The calculations were carried out for condition of bubble equilibrium, i.e. for $p = 2\gamma/r$, where p is the pressure, γ is the surface tension and r is the bubble radius. The bubbles are pre-equilibrium if $N/N_0 > 1$ and they are overpressured for $N/N_0 < 1$. Since it is known that the quantity of helium in the crystal lattice is insignificant after formation of bubbles, it is assumed that all helium is located in the bubbles. Moreover, two factors are considered: (1) various trapping coefficients of implanted helium for different temperatures and steels [3]; (2) the distribution spectrum of implanted helium is Gaussian with a maximum range ~0.3 μm and projected range of about 0.15 μm. However, only the near-surface layer of thickness ~0.12 μm is observed by TEM operating at 200 kV.

Thus, bubbles formed at 900 K are pre-equilibrium and bubbles obtained at other implantation temperatures are overpressured for both steels investigated (Table 1).

The quantity of retained hydrogen in the steels with different types of helium bubbles is presented in Table 2. As can be seen from the table, a considerably greater quantity of hydrogen is retained in initial (unirradiated by He^+) samples than that in samples with a preliminary implanted by helium. More hydrogen remains in He^+-irradiated EP-900 steel in the absence of helium bubbles ($T_{irrad} = 570$ K) than in samples with helium porosity. At the same time, the quantity of retained hydrogen increases with a decrease of the helium pressure in the bubbles for both types of steels. In addition, much more hydrogen is retained in austenitic steel with a previously created helium porosity and there is a greater increase of the quantity of trapped hydrogen with increasing irradiation temperature (i.e. with decreasing the helium pressure in the bubbles) compared to the EP-900 steel.

As shown above, the preferred helium porosity evolution in EP-900 steel (as well as for other 13%Cr-type steels [6]) is formation and growth of bubbles on dislocations and dislocation nodes (Fig. 2), in contrast to Cr18Ni10Ti steel which has a homogeneous distribution of bubbles in the matrix (Fig. 1). This distinction in the bubble evolution may be the main reason for the helium bubbles not being effective traps for hydrogen in the BCC lattice, as hydrogen atoms absorbed by helium bubbles can easily leave the samples along the dislocations [12]. This does not contradict literature data [8–10] which show that helium bubbles are able to retain hydrogen, as these results are mainly for austenitic steels, obtained under a sequential implantation of helium and hydrogen into the austenitic materials with a homogeneous development of helium bubbles in the matrix.

The results of this work show that small overpressured helium bubbles are not effective traps for hydrogen, and in addition they are able to facilitate the release of hydrogen from samples. Microstructural components of steels (for example, structural defects, second phase boundaries, etc.), as well as radiation-induced defects produced by

Table 2
Hydrogen content in samples of EP-900 and Cr18Ni10Ti steels sequentially irradiated with He^+- and H^+-ions

Steel	He^+-ion irradiation temperature (K)	Character of helium bubbles	Hydrogen content, in wt%
EP-900	Without irradiation	No bubbles	0.00890
	570	Different types of helium–vacancy complexes	0.00140
	690	Probably, the smallest overpressured bubbles	0.00077
	770	Overpressured bubbles	0.00082
	900	Pre-equilibrium bubbles	0.00098
Cr18Ni10Ti	Without irradiation	No bubbles	0.00830
	570	Different type of helium–vacancy complexes (probably, the smallest overpressured bubbles)	0.00189
	690	The smallest overpressured bubbles	0.00205
	770	Overpressured bubbles	0.00234
	900	Pre-equilibrium bubbles	0.00388

He^+-irradiation are strong traps for hydrogen (Table 2). Comparing ferritic–martensitic and austenitic steels, it is concluded that the austenitic steel with a uniform distribution of helium bubbles retain a greater quantity of hydrogen than the ferritic–martensitic steel with bubbles predominantly located on dislocations.

The helium desorption spectra of samples irradiated by He^+- and H^+-ions are characterized by one intense peak for the austenitic steel and by two intense peaks for the ferritic–martensitic steel [13] and by some difficult-to-resolute additional peaks. It is well known [3,14] that at a fluence of irradiation by He^+-ions up to $5 \times 10^{20}\ m^{-2}$, the release of helium mainly occurs by the mechanism of bubble migration, coalescence during the migration and the release of bubbles from the surface, creating a 'pin-hole' structure. The characteristics of helium thermodesorption (Fig. 3) are the following: (1) the release of helium on uniform heating from ferritic–martensitic steel takes place earlier than that from austenitic steel owing to favorable bubble migration in the BCC lattice; (2) the HTDS peaks shift to higher temperature with an increase of the helium implantation temperature (see Table 1 and Fig. 3), i.e. with formation of bubbles under irradiation, the migration of large bubbles is more difficult than that of small bubbles [15]; (3) in Cr18Ni10Ti steel, the subsequent hydrogen implantation shifts the HTDS peaks to even higher temperature as a result of further bubble-sizes growth after 25-keV H^+-irradiation; this is possibly due to trapping of hydrogen by helium bubbles; (4) in case of EP-900 steel, hydrogen shifts HTDS peaks to lower temperatures, which is probably due to favorable migration and release of bubbles along the dislocations.

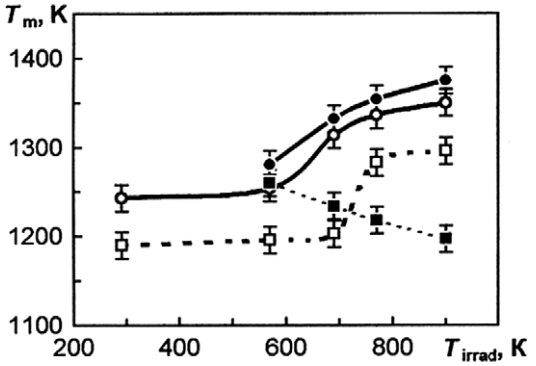

Fig. 3. Helium thermal desorption spectrometry main peak temperature as a function of the He^+-ion irradiation temperature for Cr18Ni10Ti (○, ●) and EP-900 (□, ■) steels: ○, □ – irradiation by He^+-ions; ●, ■ – irradiation by He^+-ions and consequently by H^+-ions (the uniform heating rate is 1.2 K/s).

4. Summary

Comparing ferritic–martensitic and austenitic steels, it is concluded that the austenitic steel with a uniform distribution of helium bubbles retain a greater quantity of hydrogen than the ferritic–martensitic steel with helium bubbles predominantly located on dislocations. The quantity of trapped hydrogen increases with a decrease of the helium pressure in these bubbles. It seems, structural imperfections of steels are more effective traps for hydrogen than are helium bubbles.

References

[1] F.A. Garner, L.R. Greenwood, D.L. Harrod, in: Proceedings of the VI International Symposium on Environmental Degradation of Material in Nuclear Power Systems – Water Reactors, The Minerals, Metals & Materials Society, 1993, p. 783.

[2] F.A. Garner, L.R. Greenwood, Radiat. Eff. Defects Solids 144 (1998) 251.
[3] B.A. Kalin, I.I. Chernov, A.N. Kalashnikov, M.N. Esaulov, Problems Atomic Sci. Ser.: Radiat. Damage Phys. Radiat. Mater. Sci. 1/2 (65/66) (1997) 53.
[4] S.Yu. Binyukova, B.A. Kalin, A.N. Kalashnikov, I.I. Chernov, Perspective Mater. 4 (2002) 50 (in Russian).
[5] S.Yu. Binyukova, I.I. Chernov, B.A. Kalin, et al., Atom. Energy 93 (2002) 32 (in Russian).
[6] I.I. Chernov, A.N. Kalashnikov, B.A. Kalin, S.Yu. Binyukova, J. Nucl. Mater. 323 (2003) 341.
[7] J.W. Edington, Practical Electron Microscopy in Materials Science. Part 4: Typical Electron Microscope Investigations, Macmillan Press Ltd., London, 1976.
[8] I.M. Nekludov, G.D. Tolstolutskaya, Problems Atomic Sci. Ser.: Radiat. Damage Phys. Radiat. Mater. Sci. 3 (2003) 3.
[9] G.D. Tolstolutskaya, V.V. Ruzhitsky, I.E. Kopanets, et al., Problems Atomic Sci. Ser.: Radiat. Damage Phys. Radiat. Mater. Sci. 3 (2004) 3.
[10] J.D. Hunn, M.B. Lewis, E.H. Lee, in: Proceedings of II International Topical Meeting on Application of Accelerator Technology, 1998, p. 375.
[11] S.E. Donnelly, Radiat. Eff. 90 (1985) 1.
[12] A.G. Zaluzhny, V.P. Kopytin, A.V. Markin, et al., Problems Atomic Sci. Ser.: Radiat. Damage Phys. Radiat. Mater. Sci. 1 (52) (1990) 51.
[13] I.I. Chernov, S.Yu. Binyukova, B.A. Kalin, et al., J. Nucl. Mater., these Proceedings, doi:10.1016/j.jnucmat.2007.03.115.
[14] V.F. Zelenskij, I.M. Nekludov, V.V. Ruzhitskij, et al., J. Nucl. Mater. 151 (1987) 22.
[15] K. Ono, K. Arakawa, M. Oohashi, et al., J. Nucl. Mater. 283–287 (2000) 210.